Oxidative Dehydrogenation of Isobutane to Isobutene on Metal-doped MCM-41 Catalysts

Takuya EHIRO[1], Ai ITAGAKI[1], Hisanobu MISU[1], Masashi KURASHINA[2], Keizo NAKAGAWA[3,4], Masahiro KATOH[3], Yuuki KATOU[5], Wataru NINOMIYA[5] and Shigeru SUGIYAMA[3,4]

[1]*Department of Chemical Science and Technology, Tokushima University, Minamijosanjima, Tokushima-shi, Tokushima 770-8506, Japan*

[2]*Department of Life System, Institute of Technology and Science, Tokushima University, Minamijosanjima, Tokushima-shi, Tokushima 770-8506, Japan*

[3]*Department of Advanced Materials, Institute of Technology and Science, Tokushima University, Minamijosanjima, Tokushima-shi, Tokushima 770-8506, Japan*

[4]*Department of Resource Circulation Engineering, Center for Frontier Research of Engineering, Tokushima University, Minamijosanjima, Tokushima-shi, Tokushima 770-8506, Japan*

[5]*Otake Research Laboratories, Mitsubishi Rayon Co. Ltd., 20-1, Miyuki-cho, Otake-shi, Hiroshima 739-0693, Japan*

Keywords: Oxidative Dehydrogenation, Isobutane, Isobutene, MCM-41, Metal-Doping

Abstract

MCM-41 (#41 Mobil Composition of Matter) is a favorable material for heterogeneous reactions because of its unique porous structure. However, the catalytic activity of MCM-41 for the oxidative dehydrogenation (ODH) of isobutane to isobutene is known to be quite low. In the present study, a metal-doping method was employed to improve this catalytic activity. Doping of Cr, Co, Ni, or Mo into MCM-41 resulted in a great improvement in the catalytic activity. Since chromium-doped MCM-41 (Cr-MCM-41) showed the greatest catalytic activity among these catalysts, its redox property was further analyzed via XPS, XAFS and H_2-TPR techniques. The XPS spectrum of Cr-MCM-41 suggested that it has Cr^{3+} and Cr^{6+} species on its surface. Also, a pre-edge peak due to Cr^{6+} species was confirmed in the XANES spectrum of Cr-MCM-41. In H_2-TPR measurement, Cr-MCM-41 was more reducible than crystalline Cr_2O_3, which showed low catalytic activity for the ODH of isobutane. The reducible Cr^{6+} species on Cr-MCM-41 contributed to an improvement in the catalytic activity of MCM-41.

Introduction

Lower olefins are valuable raw materials for various products. Currently, naphtha-cracking process is a major production method for lower olefins, but this process suffers from severe operating conditions such as a huge amount of energy consumption and difficulties in controlling the product composition (Yoshiura *et al*., 2000). To produce lower olefins more efficiently, oxidative coupling of methane (Sekine *et al*., 2009), metathesis reaction (Iwamoto *et al*., 2008), dehydrogenation (Liebmann and Schmidt, 1999; Wang *et al*., 2001) and oxidative dehydrogenation (Santamaría-González *et al*., 2000; Neri *et al*., 2004; Nakamura *et al*., 2006; Wang *et al*., 2009) have recently been investigated. Although the dehydrogenation of lower paraffin is an industrialized reaction process, its endothermic reaction requires a high reaction temperature and the regeneration of a catalyst in a rapid cycle. In contrast, oxidative dehydrogenation (ODH) is an exothermic reaction. Therefore, ODH has the potential to be a highly energy-efficient reaction. Also, the oxygen of the reactant would be expected to prevent the rapid deactivation of a catalyst due to coke deposition. In the present study, the ODH of isobutane was conducted for an efficient synthesis of isobutene, which is a useful chemical ingredient for the production of either methyl tertiary butyl ether (Eldarsi *et al*., 1998) or methyl methacrylate (Nagai, 2001; Kuroda, 2003).

In the past, various metal oxide catalysts have been used to catalyze the ODH of isobutane (Jibrila *et al*., 2005). There are more reports of unsupported or supported chromia catalysts than that of catalysts containing other metals (Grabowski *et al*., 1996; Grzybowska *et al*., 1998; Al-Zahrani *et al*., 2001; Neri *et al*., 2004; Jibrila *et al*., 2005; Wang *et al*., 2009; Zhang *et al*., 2009), presumably because some Cr species were originally found to be suitable for the ODH of isobutane. Previously, our research group attempted the preparation of Cr-doped mesoporous silica catalysts based on FSM-16 (#16 Folded Sheet Mesoporous Material), and this showed great catalytic activity for the ODH of isobutane (Sugiyama *et al*., 2013). These attempts succeeded in preparing catalytically active Cr-doped silica catalysts, which attained a more than 8% isobutene yield. However, it was confirmed that although their porous structures were characteristic of mesoporous silica, they were partially destroyed (Sugiyama *et al*., 2013).

To obtain porous catalytically active catalysts, a template ion exchange (TIE) method (Iwamoto and Tanaka, 2001) was applied to another mesoporous silica, MCM-41 (#41 Mobil Composition of Matter)

Correspondence concerning this article should be addressed to S. Sugiyama (E-mail address: sugiyama@tokushima-u.ac.jp).

(Kresge *et al*., 1992), in the present study. Although there are the limitations in applicability, the TIE method has the following advantages when introducing metal species into a mesoporous silica (Iwamoto and Tanaka, 2001): (1) the ordered porous structure remains even after metal-doping; (2) it is possible to control the metal loading weight; (3) metal species can be dispersed on the surface; and, (4) the TIE method can be used to introduce various metal species. MCM-41 also has desirable features for catalytic activity. Its mesoporous channels provide a wide reaction field, which is favorable for adsorption, desorption and diffusion of gases, and its thermal stability is sufficient for use in the ODH of isobutane. Therefore, the objective of the present study was to prepare catalytically active and mesoporous metal-doped catalysts via the TIE method. In addition to doping with Cr, metals belonging to the same group or period, V, Mn, Fe, Co, Ni, Cu, and Mo, were introduced to MCM-41 in a search for the best combination of a metal and MCM-41.

1. Experimental

1.1 Catalyst preparation

In the preparation of MCM-41, the hydrothermal synthesis method reported by Iwamoto and his colleague (Iwamoto *et al*., 2000) was applied in the present study. Dodecyltrimethylammonium bromide (33.8 g (109 mmol), Wako Pure Chemical Industries, Ltd.) dissolved in 96.2 g of distilled water and 45.9 g of colloidal silica (Snowtex 20, Nissan Chemical Ind.) were used as the surfactant template and the silica source, respectively. Sodium hydroxide (1.74 g (43.5 mmol), Wako Pure Chemical Industries, Ltd.) was dissolved into 18.8 g of distilled water and used for pH adjustment of the solution. Colloidal silica and sodium hydroxide were alternatively dropwise added to the surfactant solution for about 20 min, and the mixed solution was stirred at 313 K for 2 h. The pH of the mixed solution was confirmed at approximately 11.5 after about 2 h of stirring. The hydrothermal synthesis was carried out at 413 K for 48 h without stirring. The obtained white wet solid was filtered, washed with distilled water, and dried at 333 K. The dried white powder was denoted as "As-synthesized MCM-41." Finally, MCM-41 was obtained by calcination at 873 K for 6 h.

Metal-doping was carried out via the TIE method (Yonemitsu *et al*., 1997; Iwamoto and Tanaka, 2001). In this work, the V, Cr, Mn, Fe, Co, Ni, Cu, and Mo were introduced to MCM-41 as follows. As-synthesized MCM-41 (2 g) was dispersed in 20 g of distilled water, while a metal source that contained 42.6 mmol of a metal element was dissolved in another 20 g of distilled water. Then, the metal precursor aqueous solution was added to the slurry of MCM-41 and stirred vigorously for 1 h. The mixed solution was heated at 353 K for 20 h without stirring. The resultant mixture was filtered, washed with distilled water, and dried at 333 K. Finally, metal-doped MCM-41 was obtained by calcination at 823 K for 6 h. The final metal-doped MCM-41 was denoted as M-MCM-41 (M = V, Cr, Mn, Fe, Co, Ni, Cu, or Mo). The metal precursors used for doping are listed in **Table 1**. The colors of the as-synthesized and calcined M-MCM-41 catalysts also are described in Table 1.

1.2 Catalyst characterization

The structural properties of the catalysts were analyzed via X-ray diffraction (XRD; RINT 2500X, Rigaku Co.), N_2 adsorption measurement (BELSORP-18SP, Bel Japan Inc.), and a transmission electron microscope (TEM; JEM-2100F, JEOL Ltd.). The powder XRD patterns of the catalysts were obtained using monochromatized Cu Kα radiation (40 kV, 40 mA). Before the N_2 adsorption measurement at 77 K, the catalysts were pretreated at 473 K for 10 h in a vacuum. The TEM images of the mesoporous catalysts were obtained at an accelerating voltage of 200 kV.

The redox properties and chemical states of the Cr species were evaluated via X-ray photoelectron spectroscopy (XPS; PHI-5000VersaProbe II, ULVAC-PHI Inc.), an H_2 temperature-programmed reduction (TPR; BELCAT-A, Bel Japan Inc.) technique, X-ray absorption fine structure (XAFS) measurement performed with Synchrotron radiation at the beam-line NW9A station of the Photon Factory in the High Energy Accelerator Research Organization (Tsukuba, Japan), and Raman spectroscopy (SH0056, Renishaw inVia Raman microscope). The XPS spectra of the catalysts

Table 1 Metal precursors and the colors of as-synthesized and calcined metal-doped MCM-41

Catalyst	Metal precursor	Maker	Metal precursor used [g]	Metal content [wt%]	Color of M-MCM-41	
					As-synthesized	Calcined
V-MCM-41	$VOC_2O_4 \cdot nH_2O$	Wako Pure Chemical Industries	0.090	1.8	Green	Yellow
Cr-MCM-41	$Cr(NO_3)_3 \cdot 9H_2O$	Sigma-Aldrich Japan	0.170	1.8	Green	Yellow
Mn-MCM-41	$(CH_3COO)_2Mn \cdot 4H_2O$	Wako Pure Chemical Industries	0.104	1.8	Reddish brown	Reddish brown
Fe-MCM-41	$Fe(NO_3)_3 \cdot 9H_2O$	Kanto Chemical Co.	0.258	2.7	Orange	Reddish brown
Co-MCM-41	$Co(NO_3)_2 \cdot 6H_2O$	Wako Pure Chemical Industries	0.124	2.0	Pink	Purple
Ni-MCM-41	$Ni(NO_3)_2 \cdot 6H_2O$	Wako Pure Chemical Industries	0.124	2.0	Pale green	Pale orange
Cu-MCM-41	$Cu(NO_3)_2 \cdot 3H_2O$	Wako Pure Chemical Industries	0.129	2.2	Light blue	Light blue
Mo-MCM-41	$(NH_4)_6Mo_7O_{24} \cdot 4H_2O$	Kanto Chemical Co.	0.113	0.4	White	White

were recorded from 570 eV to 590 eV. They were calibrated based on the C 1s peak at 285.0 eV. H_2-TPR measurement was carried out flowing 40 sccm 5% H_2/Ar gas from 373 to 1,073 K at a rate of 10 K/min. The amount of H_2 consumption was detected via TCD. Water in the produced gas was trapped with a molecular sieve 13X before the gas had passed through the TCD. Each catalyst (50 mg) was exposed to a pretreatment of 50 sccm Ar gas flow at 773 K for 1 h before flowing 40 sccm 5% H_2/Ar gas. Raman spectra of Cr-containing samples were recorded by using a laser excitation wavelength of 532 nm.

The Cr content in the catalyst was calculated by analyzing the concentration of chromium ion in the remaining solution from the synthesis by ICP-AES (SPS3520UV, SII Nanotechnology).

1.3 Catalytic activity test

The catalytic activity tests were carried out in a fixed-bed continuous flow reactor at atmospheric pressure. Each catalyst (0.25 g) was pelletized and sieved to 0.85–1.70 mm. They were fixed with quartz wool and pretreated with 12.5 mL/min of O_2 gas flow at 723 K. After the pretreatment, catalytic activity tests were started by flowing 15 mL/min of helium, isobutane and oxygen to the reactor. Their partial pressures were adjusted to P(He) = 74.6 kPa, P(i-C_4H_{10}) = 14.4 kPa, and P(O_2) = 12.3 kPa, respectively. These reaction conditions were used unless otherwise stated. Under these conditions, a homogeneous gas phase reaction was not observed, but stable activity was observed for up to 6 h on-stream.

The reaction was monitored using an online gas chromatograph (Shimadzu GC-8APT) equipped with a TCD. A Molecular Sieve 5A (MS 5A, 0.2 m×Φ3 mm) for O_2, CH_4 and CO and a Hayesep R (2.0 m×Φ3 mm) for CO_2, C2, C3, and C4 products were used as the columns. The carbon balance between the reactant and the products was within ± 5 %. The product selectivity and isobutane conversion were calculated on a carbon basis.

2. Results and Discussion

2.1 Structural properties

Figure 1 (A) shows the XRD patterns of MCM-41, 1.8 wt% Cr-MCM-41, and 2.7 wt% Fe-MCM-41. The diffraction peaks of MCM-41 between 2θ = 2-5.5° were assigned to the (100), (110) and (200) planes of a 2D hexagonal ordered structure (Wang *et al*., 2003). These diffraction peaks are characteristic of MCM-41, they remained after the introduction of the other metals, although those of 2.7 wt% Fe-MCM-41 were weakened. Therefore, the metal-doped MCM-41 catalysts had mesoporous-ordered hexagonal structures. The first peak assigned to the (100) plane was used to calculate the lattice constant, as listed in **Table 2**. The XRD

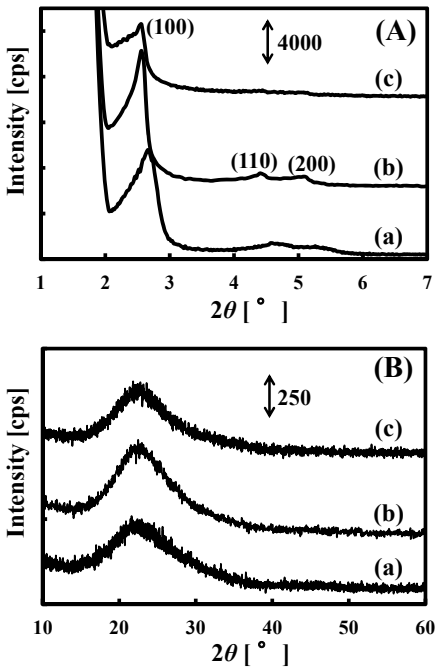

Fig. 1 XRD patterns of (a) MCM-41, (b) 1.8 wt% Cr-MCM-41 and (c) 2.7 wt% Fe-MCM-41 at (A) low and (B) high diffraction angle

Table 2 Parameters obtained from XRD, surface area and total pore volume of MCM-41 and metal-doped MCM-41 catalysts

Catalyst	2θ [°]	d_{100} [Å]	a_0 [Å]	BET surface area [m^2/g]	Total pore volume [cm^3/g]
MCM-41	2.66	33.19	38.32	788	0.61
1.8 wt% V-MCM-41	2.52	35.03	40.45	808	0.67
1.8 wt% Cr-MCM-41	2.56	34.48	39.81	781	0.75
1.8 wt% Mn-MCM-41	2.54	34.75	40.13	783	0.71
2.7 wt% Fe-MCM-41	2.56	34.48	39.81	688	0.81
2.0 wt% Co-MCM-41	2.54	34.75	40.13	809	0.79
2.0 wt% Ni-MCM-41	2.54	34.75	40.13	997	1.10
2.2 wt% Cu-MCM-41	2.58	34.22	39.51	897	0.84
0.4 wt% Mo-MCM-41	2.56	34.48	39.81	858	0.72

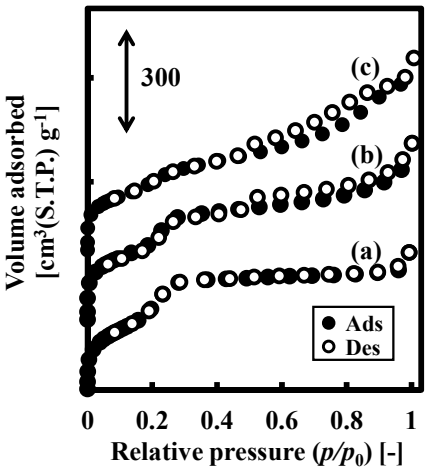

Fig. 2 N_2 adsorption-desorption isotherms of (a) MCM-41, (b) 1.8 wt% Cr-MCM-41 and (c) 2.7 wt% Fe-MCM-41 (The starting point of each isotherm is different)

patterns for the high diffraction angles are shown in **Figure 1 (B)**. The broad peak at approximately $2\theta = 22°$ was due to the amorphous silica walls of MCM-41. In all the metal-doped MCM-41 catalysts, no peak could be ascribed to metal oxide.

The structural properties of the metal-doped MCM-41 catalysts were also evaluated via N_2 adsorption measurement. All N_2 adsorption-desorption isotherms could be classified as a type IV. There was a plateau region for the N_2 adsorption-desorption isotherm of MCM-41 after capillary condensation (p/p_0 = 0.3-0.9) (**Figure 2 (a)**). However, the plateaus for 1.8 wt% Cr-MCM-41 and 2.7 wt% Fe-MCM-41 had more slope than that of MCM-41 (**Figure 2 (b)** and **(c)**). The same tendency was observed for the N_2 adsorption-desorption isotherm of the other metal-doped MCM-41 catalysts (not shown). The increase in the amount adsorbed after the capillary condensation (p/p_0 = 0.3–0.9) may suggest that the metal-doped MCM-41 catalysts had less-ordered hexagonal pores compared with those of MCM-41. As discussed in the previous report (Sugiyama *et al*., 2010), an ion exchange between the Si^{4+} of the silica wall and the metal ion may have occurred and distorted the mesoporous channels. From this viewpoint, it could be assumed that the incorporation of some metal ions into the silica wall widened the mesopore, resulting in an increase in the lattice constant, a_0. However, the distortion of the mesopores caused by metal-doping was slight, because the BET surface areas calculated from the N_2 adsorption isotherms were not dependent on the doping (Table 2).

Furthermore, the nanostructure of the 1.8 wt% Cr-MCM-41 was observed by TEM (**Figure 3**). An ordered structure could be observed in many of the nano- or micro-sized particles of 1.8 wt% Cr-MCM-41 (Figure 3 (A)). However, an amorphous-like region was also confirmed in a particle (Figure 3 (B)). In that region, the black dots shown in Figure 3 (B) were also captured. These were probably chromium oxide particles, however they were not observed in other regions. Therefore, the results of XRD and TEM analysis suggested that the doped metal species were sufficiently small or dispersed so as to be undetectable.

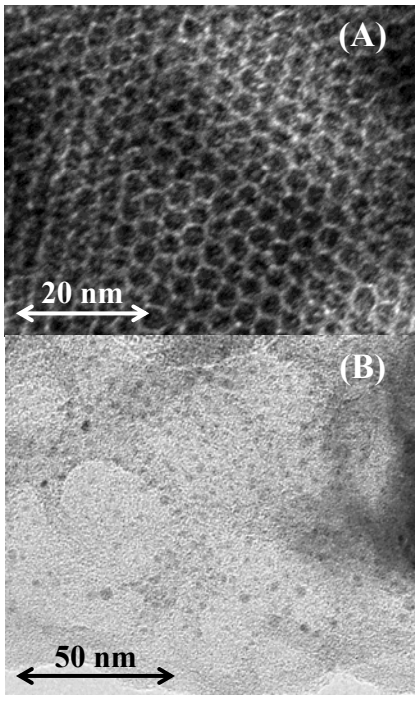

Fig. 3 TEM images of 1.8 wt% Cr-MCM-41

2.2 Catalytic activity during the oxidative dehydrogenation of isobutane

The measures of activity for each of the metal-doped MCM-41 catalysts are listed in **Table 3**. As shown in Table 3, the catalytic activity of MCM-41 was quite low. To improve this low catalytic activity, metal-doping into MCM-41 was conducted via the TIE method. Doping with V or Mn resulted in an enhancement in the conversion of isobutane, but the yield of isobutene was unchanged. Unfortunately, isobutene was not detected in Fe or Cu-doped MCM-41. Therefore, the deep oxidation of isobutene to COx may proceed via doping with Fe or Cu. However, doping with Cr, Ni, Co, or Mo into MCM-41 resulted in a great improvement in catalytic activity. Among these catalysts, 1.8 wt% Cr-MCM-41 showed the greatest isobutene yield (6.8%). In our previous study, Cr-FSM-16 was prepared via the TIE method (Sugiyama *et al*., 2013). However, the catalytic activity on Cr-FSM-16 (isobutene yield 2.8%) was lower that on 1.8 wt% Cr-MCM-41. This is probably due to a smaller amount of surfactants used in preparing FSM-16, resulting in the difficulty for the introduction of metal species into FSM-16. Hence, Cr content in Cr-FSM-16 was limited to 0.3 wt% and its redox property was hardly confirmed via the H_2-TPR, although its acidic properties were improved (Sugiyama *et al*., 2015).

Table 3 Catalytic activities for the ODH of isobutane on various catalysts at 6.0 h on-stream

Catalyst	Conversion[%]	Selectivity [%]		Yield [%]
	i-C_4H_{10}	COx	i-C_4H_8	i-C_4H_8
MCM-41	8.3	76.2	11.2	0.9
1.8 wt% V-MCM-41	17.1	81.2	10.7	1.8
1.8 wt% Cr-MCM-41	20.6	59.3	32.8	6.8
1.8 wt% Mn-MCM-41	14.7	84.7	8.2	1.2
2.7 wt% Fe-MCM-41	13.3	96.7	0	0
2.0 wt% Co-MCM-41	21.0	54.7	24.7	5.2
2.0 wt% Ni-MCM-41	21.6	67.1	23.7	5.1
2.2 wt% Cu-MCM-41	14.1	94.2	0	0
0.4 wt% Mo-MCM-41	23.0	66.4	26.9	6.2

2.3 Effects of the feed ratio of the reactants on the catalytic activity

Comparisons of the catalytic activities of metal-doped MCM-41 catalysts showed that Cr-doping was the most effective way to improve the catalytic activity of MCM-41. Therefore, the remainder of this article

focuses on Cr-MCM-41. In order to examine the effect of the feed ratio (i-C_4H_{10}/O_2) on catalytic activity, 1.8 wt% Cr-MCM-41 was tested in different feed ratios.

Figure 4 shows the catalytic activities for 1.8 wt% Cr-MCM-41 at different feed ratios. With an increase in the feed ratio, the conversion of isobutane and the selectivity to COx decreased while the selectivity to isobutene increased, as observed in the typical partial oxidation of various alkanes. The maximum yield of isobutene, therefore, was obtained at a feed ratio of 1.2 during testing in the present study. It should be noted that the greatest selectivity of isobutene (92%) was

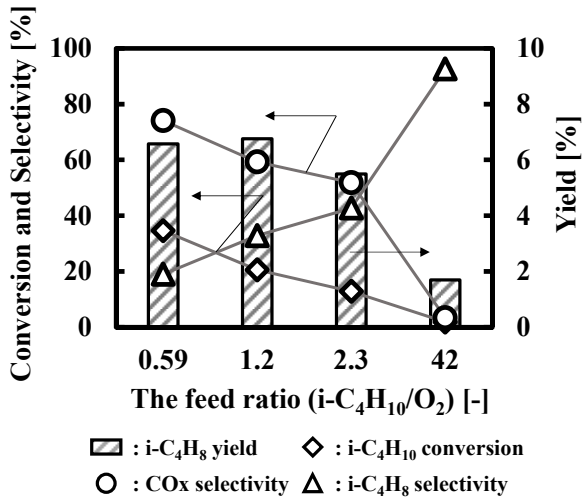

Fig. 4 Catalytic activities for the ODH of isobutane on 1.8 wt% Cr-MCM-41 at different feed ratios and 6 h on-stream

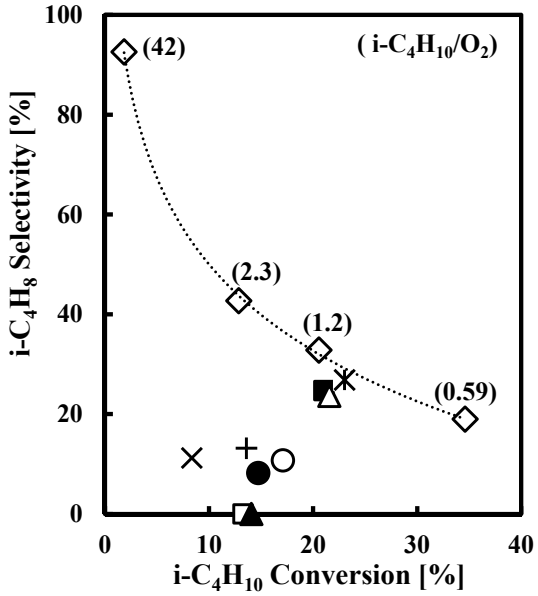

Fig. 5 Isobutene selectivity versus isobutane conversion of 1.8 wt% Cr-MCM-41 (◇) at different i-C_4H_{10}/O_2 ratios (0.59, 1.2, 2.3, or 42), M-MCM-41 (M = V (○), Mn (●), Fe (□), Co (■), Ni (△), Cu (▲), and Mo (✻)), MCM-41 (×), and α-Cr_2O_3 (+) at i-C_4H_{10}/O_2 ratio = 1.2, 723 K, and 6.0 h on-stream

detected at a feed ratio of 42, while the conversion of isobutane was less than 9% under these conditions at 6 h on-stream, which resulted in the lowest yield of isobutene in the present study.

In **Figure 5,** isobutene selectivities on all catalysts at 6 h on-stream were plotted versus the corresponding isobutane conversions using data shown in Table 3. Furthermore, the catalytic activities at different feed ratios (0.59, 1.2, 2.3, and 42) were also plotted for 1.8 wt% Cr-MCM-41 and connected using the dashed line. Although 0.4 wt% Mo-MCM-41 showed almost same activity to that on 1.8 wt% Cr-MCM-41, it was found that 1.8 wt% Cr-MCM-41 showed the greatest catalytic activity among these M-MCM-41 catalysts.

2.4 Redox properties of Cr-MCM-41

To reveal active sites on Cr-MCM-41, which showed the greatest catalytic activity, the catalytic activity during the ODH of the isobutane in crystalline α-Cr_2O_3 (Wako Pure Chemical Industries, Ltd.) was also tested under standard conditions. Compared with the isobutene yield of 1.8 wt% Cr-MCM-41 (Table 3), that of crystalline α-Cr_2O_3 was much lower (1.8%) at 6 h on-stream, which showed that Cr-MCM-41 possesses catalytically active and distinctive chromium species. The Cr^{6+} species on either Ca-doped $CrOx/Al_2O_3$ or CrOx/SBA-15 selectively catalyzed the ODH of isobutane (Neri *et al*., 2004; Wang *et al*., 2009). However, it is conceivable that an active chromium species would be reduced and inactive while catalyzing the reaction. A previous report (Takita *et al*., 2005) proposed that oxygen plays a crucial role in oxidizing Ce^{3+} and changing it to Ce^{4+}, which is a catalytically active species in the ODH of isobutane. We assume that a reduced chromium species during the reaction could also be oxidized by oxygen. To investigate the redox properties of Cr-MCM-41, which are the most important factors in establishing a stable redox cycle for chromium species, XPS, XAFS and H_2-TPR measurements were carried out for samples containing Cr.

Figure 6 (A) shows the reducibility of V, Cr or Cu-MCM-41 evaluated via the H_2-TPR technique. The peak at the low temperature showed that 2.2 wt% Cu-MCM-41 was very reducible **(Figure 6 (A) (c))**. This reducibility of 2.2 wt% Cu-MCM-41 was too strong to selectively catalyze the ODH of isobutane, resulting in the conversion of isobutane to COx. As shown in **Figure 6 (A) (a)**, 1.8 wt% V-MCM-41 showed a reducibility that was weaker than that of either 2.2 wt% Cu-MCM-41 (Figure 6 (A) (c)) or 1.8 wt% Cr-MCM-41 (**Figure 6 (A) (b)**). However, the COx selectivity of 1.8 wt% V-MCM-41 was higher than that of 1.8 wt% Cr-MCM-41 (Table 3). Therefore, the reaction mechanism for the ODH of isobutane would be decided by not only the reducibility of the catalyst, but by the nature of the active species. Next, the reducibility of 1.8 wt% Cr-

MCM-41 was compared with that of crystalline α-Cr_2O_3, which had the same active species, chromium oxide. Common peaks were observed at ca. 733 K in the TPR spectra of crystalline α-Cr_2O_3 and 1.8 wt% Cr-MCM-41 (**Figure 6 (B)**). These peaks could be attributed to Cr^{3+} species with low degrees of polymerization (Santamaría-González *et al*., 2000). No broad peak for crystalline α-Cr_2O_3 could be observed in the high temperature region (> 770 K) in the TPR spectra of Cr-MCM-41 (**Figure 6 (B) (a)–(c)**). The broad peak was assigned to highly aggregated polychromate species or crystalline Cr_2O_3 (Wang *et al*., 2009). In contrast, the TPR spectra of 1.8 wt% Cr-MCM-41 showed its characteristic peak in a lower temperature region, although the peak was weakened by the pretreatment at 723 K for 1 h (Figures 6 (B) (b) and (c)). Based on these results, it was concluded that 1.8 wt% Cr-MCM-41 was more reducible than crystalline α-Cr_2O_3. Since crystalline α-Cr_2O_3 was inactive for the ODH of isobutane, as mentioned above, the stronger degree of its reducibility was an important factor in the great catalytic activity of Cr-containing catalysts.

The XPS spectra of crystalline α-Cr_2O_3 and 1.8 wt% Cr-MCM-41 were obtained (**Figure 7**). The shape of an XPS spectrum usually depends on the elements on the surface and on their oxidation state. Because crystalline α-Cr_2O_3 is mainly composed of Cr^{3+} species, its peaks were mainly attributed to Cr^{3+} species. As shown in **Figures 7 (a)** and **(b)**, the shape in the XPS spectrum of crystalline α-Cr_2O_3 was different from that of 1.8 wt% Cr-MCM-41, which indicated that different oxidation states of chromium species were present in both catalysts. A paper reported by Wang *et al*. (2009) was used as the standard for peak positions (Figure 7), which eased the task of separating the peaks of the XPS spectra into Cr^{3+} and Cr^{6+}. Based on that report, Cr $2p_{3/2}$ and $2p_{1/2}$ due to Cr^{3+} were detected at 576.5 and 585.5 eV while those due to Cr^{6+} were seen at 587.5 and 579.0 eV, respectively. Comparing the XPS spectra with the standard peak positions, it appeared that there were fewer Cr^{6+} species on crystalline α-Cr_2O_3. On the contrary, there were much greater number of Cr^{6+} species on Cr-MCM-41 because the tops of its peaks had shifted to a higher binding energy, which showed that there were Cr^{3+} and Cr^{6+} species on Cr-MCM-41. When the 1.8 wt% Cr-MCM-41s were measured by XPS after the ODH of isobutane and after O_2 treatment with 12.5 mL/min of O_2 gas flow at 723 K for 2 h, there were no significant differences in their XPS spectra (**Figures 7 (b)–(d)**). Since 1.8 wt% Cr-MCM-41 showed stable catalytic activity in the ODH of isobutane, it was understandable that the nature of the surface region on the catalyst had remained even following the ODH of isobutane.

The Cr K-edge XANES spectra of 2.2 wt% Cr-MCM-41 before and after the ODH of isobutane are described in **Figures 8 (a)** and **(b)**. In the present study, 2.2 wt% Cr-MCM-41, which showed the same catalytic activity (6.8% isobutene yield) at 6 h on-stream to that on 1.8 wt% Cr-MCM-41, was measured in order to estimate the situation of chromium species more clearly. Furthermore, 2.2 wt% Cr-MCM-41 which was treated with 12.5 mL/min O_2 flow at 723 K for 2 h was also

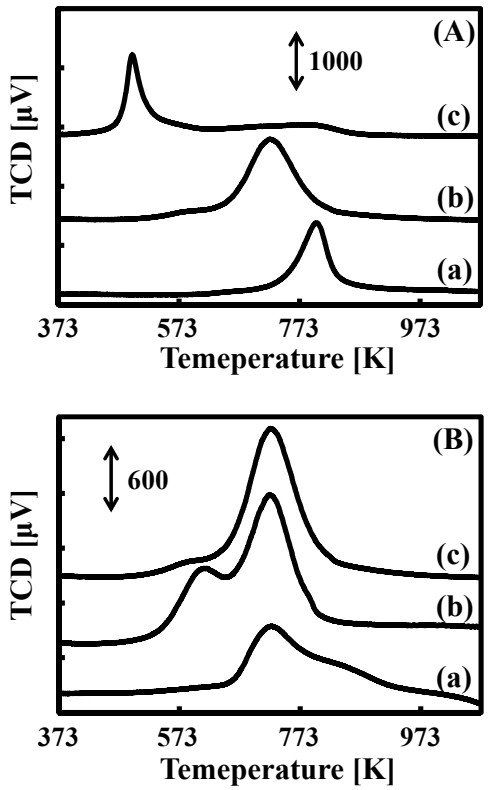

Fig. 6 TPR spectra of (A) (a) 1.8 wt% V-MCM-41, (b) 1.8 wt% Cr-MCM-41 and (c) 2.2 wt% Cu-MCM-41, and (B) (a) crystalline α-Cr_2O_3 (b) 1.8 wt% Cr-MCM-41 without the pretreatment and (c) 1.8 wt% Cr-MCM-41 with the pretreatment

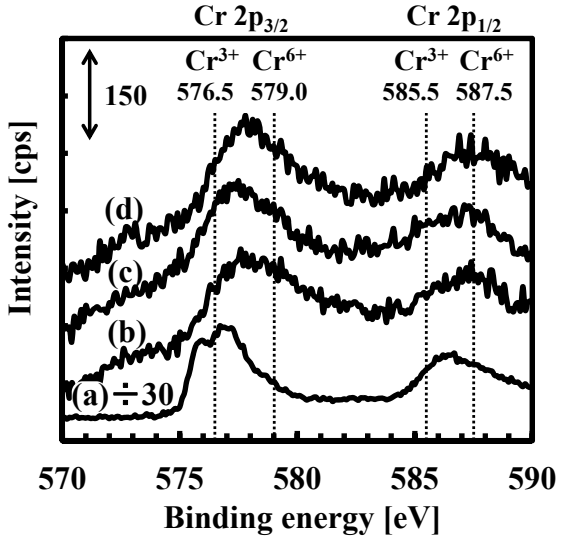

Fig. 7 XPS spectra of (a) crystalline α-Cr_2O_3, and 1.8 wt% Cr-MCM-41 (b) before ODH of isobutane, (c) after the pretreatment with O_2 flow and (d) after ODH of isobutane

analyzed to investigate the redox properties in more detail (**Figure 8 (c)**). The pre-edge peak at ca. 5991 eV represents tetrahedrally coordinated Cr^{6+} species (Wang *et al*., 2003; Takehira *et al*., 2004). The coordination state around Cr species was similar to that around the Si in MCM-41. As shown in Figures 8 (a) and (b), the intensity of the pre-edge peak was increased by O_2 treatment. Similar phenomena were observed by another research group when Cr-MCM-41 was treated with CO_2 or O_2 (Takehira *et al*., 2004), although the Cr-MCM-41 was prepared in a method that differed from ours. In the previous work (Takehira *et al*., 2004), CO_2 and O_2 were used as oxidizing agents and regenerated the reducibility and catalytic activity of Cr-MCM-41 for the dehydrogenation of propane with CO_2. In the present study, the pre-edge peak that represents tetrahedrally coordinated Cr^{6+} species were drastically reduced during the ODH of isobutane (**Figure 8 (c)**). Although

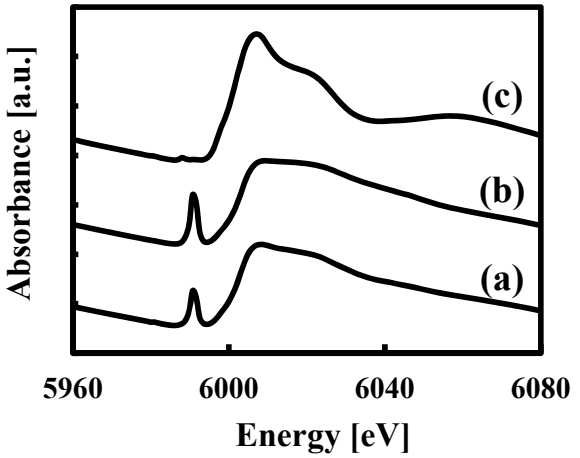

Fig. 8 Cr K-edge XANES spectra of (a) 2.2 wt% Cr-MCM-41 (a) before ODH of isobutane, (b) after the pretreatment with O_2 flow and (c) after ODH

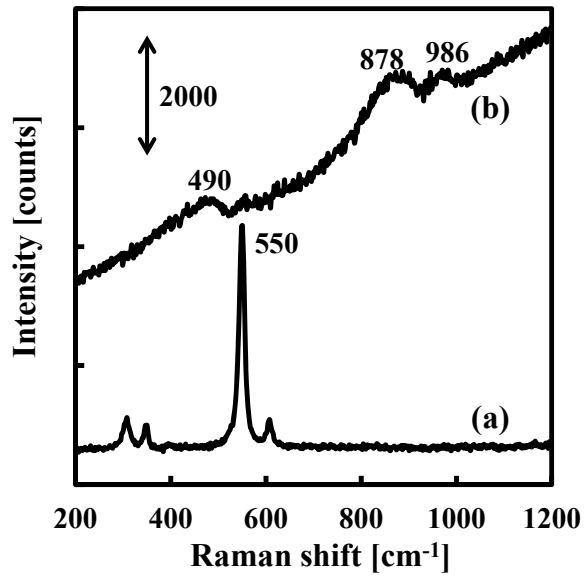

Fig. 9 Raman spectra of (a) crystalline α-Cr_2O_3 and (b) 1.8 wt% Cr-MCM-41

our Cr-MCM-41 was not deactivated during 6 h on-stream, the reduction rate of active chromium species during the ODH of isobutane might have been faster than that of their regeneration by oxygen, because the pre-edge peak disappeared. The XAFS affords information from the bulk phase but little information from the surface. As mentioned above, the XPS study did not suggest that Cr^{6+} species were reduced, because the shapes of the XPS spectra were only slightly changed (Figure 7). Therefore, the disappearance of the pre-edge peak was due to the bulk phase rather than to the surface region of the catalyst. The presence of Cr^{6+} on the surface region of the catalyst resulted in stable activity during the ODH of isobutane for at least 6 h on-stream.

Raman spectra of crystalline α-Cr_2O_3 and 1.8 wt% Cr-MCM-41 were shown in **Figure 9**. A Raman band at 550 cm^{-1} due to crystalline α-Cr_2O_3 (Wang *et al*., 2009) could not be detected in 1.8 wt% Cr-MCM-41. According to the previous report (Wang *et al*., 2009), Raman bands at 495 and 986 cm^{-1} were assignable to monochromate species of Cr^{6+} (CrO_3), while the ones in the range of 750–1010 cm^{-1} were assigned to Cr^{6+} species in the form of polychromate with different degrees of oligomerization. In the present study, the Raman bands at approximately 490, 878, and 986 cm^{-1} were detected from 1.8 wt% Cr-MCM-41. Since the Raman band at 490 cm^{-1} of 1.8 wt% Cr-MCM-41 was very close to that at 495 cm^{-1} reported for Cr^{6+} species (Wang *et al*., 2009), Raman bands at 490 and 986 cm^{-1} detected from 1.8 wt% Cr-MCM-41 could be assigned to monochromate species of Cr^{6+} state. Also, the Raman band at approximately 878 cm^{-1} was assignable to Cr^{6+} species in the form of polychromate.

According to our previous report (Sugiyama *et al*., 2015), 5.0 wt% CrOx/SiO_2 and CrOx/FSM-16, both of which were prepared via an impregnation method, showed 5.0 and 5.5% isobutene yield, respectively. These isobutene yields were lower than that of 1.8 wt% Cr-MCM-41 (6.8%). Since BET surface area of MCM-41 was higher than that of SiO_2, the aggregation of introduced metal particles may proceed on SiO_2. Furthermore, the TIE method was advantageous in dispersing metal species. Therefore, the broader Raman bands of 1.8 wt% Cr-MCM-41 might indicate that Cr species on 1.8 wt% Cr-MCM-41 are dispersed and less aggregated than those of 5.0 wt% CrOx/SiO_2 and CrOx/FSM-16. In fact, the diffraction peaks due to crystalline α-Cr_2O_3 were confirmed from 5.0 wt% CrOx/SiO_2 and CrOx/FSM-16 (Sugiyama *et al*., 2015), although they were not detected from 1.8 wt% Cr-MCM-41. Furthermore the intensity of the diffraction peaks of 5.0 wt% CrOx/SiO_2 were greater than those of 5.0 wt% CrOx/FSM-16. This indicated that mesopores of FSM-16 suppressed the aggregation of Cr species. Therefore, it was expected that aggregated Cr species, including crystalline α-Cr_2O_3 particles, on 5.0 wt%

$CrOx/SiO_2$ and CrOx/FSM-16 resulted in the decrease of the catalytic activity, compared with that on 1.8 wt% Cr-MCM-41 (Table 3). In summary, mesoporous channels of MCM-41 would provide a wider space for dispersed and catalytically active Cr^{6+} species. Furthermore, the Cr-doping via the TIE method would contribute to the formation of smaller particles of Cr^{6+} species. Therefore, it is concluded that the combination of MCM-41 and the TIE method results in the greater catalytic activity on the present systems (Table 3).

Conclusion

The TIE method produced metal-doped MCM-41 catalysts that retained the mesoporous 2D hexagonal ordered structure of MCM-41. The catalytic activity tests revealed that 1.8 wt% Cr-MCM-41 was the most catalytically active for the ODH of isobutane. The isobutene yield of MCM-41 was increased from 0.9 to 6.8% via Cr-doping. XPS and XAFS studies suggested that 1.8 wt% Cr-MCM-41 contained Cr^{6+} species. Although the pre-edge peak, which was ascribed to tetrahedrally coordinated Cr^{6+} species, disappeared following the ODH of isobutane, an XPS study suggested that many of them were retained even after the reaction. Moreover, H_2-TPR revealed that 1.8 wt% Cr-MCM-41 contained reducible chromium species. A comparison of 1.8 wt% Cr-MCM-41 with crystalline α-Cr_2O_3 showed that the quality of a reducible chromium species, as confirmed by H_2-TPR, could be ascribed to the Cr^{6+} species and active sites during the ODH of isobutane. Raman spectroscopy suggested that Cr species of 1.8 wt% Cr-MCM-41 were dispersed and Cr^{6+} species.

Acknowledgements

This work was funded by a Grant-in-Aid for Scientific Research (B) (KAKENHI 24360328) that was awarded to SS, for which we are grateful.

Literature Cited

Al-Zahrani, S. M., N. O. Elbashir, A. E. Abasaeed and M. Abdulwahed; "Catalytic Performance of Chromium Oxide Supported on Al_2O_3 in Oxidative Dehydrogenation of Isobutane to Isobutene," *Ind. Eng. Chem. Res.*, **40**, 781–784 (2001)

Eldarsi, H. S. and P. L. Douglas; "Methyl-tert-butyl-ester Catalytic Distillation Column: Part II: Optimization," *Chem. Eng. Res, Design*, **76**, 517–524 (1998)

Grabowski. R., B. Grzybowska, J. Stoczyfiski and K. Wcisto; "Oxidative Dehydrogenation of Isobutane on Supported Chromia Catalysts," *Appl. Catal. A*, **144**, 335–351 (1996)

Grzybowska, B., J. Słoczyński, R. Grabowski, K. Wcisło, A. Kozłowska, J. Stoch and J. Zieliński; "Chromium Oxide/Alumina Catalysts in Oxidative Dehydrogenation of Isobutane," *J. Catal.,* **178**, 687–700 (1998)

Iwamoto, M., T. Abe and Y. Tachibana; "Control of Bandgap of Iron Oxide through its Encapsulation into SiO_2-based Mesoporous Materials," *J. Mol. Catal. A Chem.*, **155**, 25–36 (2000)

Iwamoto, M. and Y. Tanaka; "Preparation of Metal Ion-planted Mesoporous Silica by Template Ion-exchange Method and Its Catalytic Activity for Asymmetric Oxidation of Sulfide," *Catal. Surv. Japan*, **5**, 25–36 (2001)

Iwamoto, M.; "Conversion of Ethene to Propene on Nickel Ion-loaded Mesoporous Silica Prepared by the Template Ion Exchange Method," *Catal Surv Asia*, **12**, 28–37 (2008)

Jibrila, B. Y., N. O. Elbashir, S. M. Al-Zahrani and A. E. Abasaeed; "Oxidative Dehydrogenation of Isobutane on Chromium Oxide-based Catalyst," *Chem. Eng. Process.*, **44**, 835–840 (2005)

Kresge, C. T., M. E. Leonowicz, W. J. Roth, J. C. Vartul and J. S. Beck; "Ordered Mesoporous Molecular Sieves Synthesized by a Liquid-crystal Template Mechanism," *Nature*, **359**, 710–712 (1992)

Kuroda, T.; "Development of Industrial Processes for MMA Production," *Catal. Catal.*, **45**, 366–371 (2003)

Liebmann, L. S. and L.D. Schmidt; "Oxidative Dehydrogenation of Isobutane at Short Contact Times," *Appl. Catal. A*, **179**, 93–106 (1999)

Nagai, K.; "New Development of the Production of Methyl Methacrylate," *Appl. Catal. A,* **221**, 367–377 (2001)

Nakamura, K.-I., T. Miyake, T. Konishi and T. Suzuki; "Oxidative Dehydrogenation of Ethane to Ethylene over NiO Loaded on High Surface Area MgO," *J. Mol. Catal. A,* **260**, 144–151 (2006)

Neri, G., A. Pistone, S. De Rossi, E. Rombic, C. Milone and S. Galvagno; "Ca-doped Chromium Oxide Catalysts Supported on Alumina for the Oxidative Dehydrogenation of Isobutane," *Appl. Catal. A*, **260**, 75–86 (2004)

Santamaría-González, J., J. Mérida-Robles, M. Alcántara-Rodríguez, P. Maireles-Torres, E. Rodríguez-Castellón and A. Jiménez-López; "Catalytic Behaviour of Chromium Supported Mesoporous MCM-41 Silica in the Oxidative Dehydrogenation of Propane," *Catal. Lett.*, **64**, 209–214 (2000)

Sekine, Y., K. Tanaka, M. Matsukata and E. Kikuchi; "Oxidative Coupling of Methane on Fe-Doped La_2O_3 Catalyst," *Energy Fuels*, **23**, 613–616 (2009)

Sugiyama, S., Y. Kato, T. Wada, S. Ogawa, K. Nakagawa and K.-I. Sotowa; "Ethanol Conversion on MCM-41 and FSM-16, and on Ni-Doped MCM-41 and FSM-16 Prepared without Hydrothermal Conditions," *Top. Catal.*, **53**, 550–554 (2010)

Sugiyama, S., Y. Nitta, Y. Furukawa, A. Itagaki, T. Ehiro, K. Nakagawa, M. Katoh, Y. Katou, S. Akihara and W. Ninomiya; "Oxidative Dehydrogenation of Isobutane to Isobutene on FSM-16 Doped with Cr and Related Catalysts," *J. Chem. Chem. Eng.*, **7**, 1014–1020 (2013)

Sugiyama, S., T. Ehiro, Y. Nitta, A. Itagaki, K. Nakagawa, M. Katoh, Y. Katou, S. Akihara and W. Ninomiya; "Acidic Properties of Various Silica Catalysts Doped with Chromium for the Oxidative Dehydrogenation of Isobutane to Isobutene," *J. Chem. Chem. Eng.*, **48**, 133–140 (2015)

Takehira, K., Y. Ohishi, T. Shishido, T. Kawabata, K. Takaki, Q. Zhang and Y. Wang; "Behavior of Active Sites on Cr-MCM-41 Catalysts during the Dehydrogenation of Propane with CO_2," *J. Catal.*, **224**, 404–416 (2004)

Takita, Y., X. Qing, A. Takami, H. Nishiguchi and K. Nagaoka; "Oxidative Dehydrogenation of Isobutane III. Reaction Mechanism over $CePO_4$ Catalyst," *Appl. Catal. A. Gen*., **296**, 63–69 (2005)

Wang, G., L. Zhang, J. Deng, H. Dai, H. He and C. T. Au; "Preparation, Characterization, and Catalytic Activity of Chromia Supported on SBA-15 for the Oxidative Dehydrogenation of Isobutane," *Appl. Catal. A*, **355**, 192–201 (2009)

Wang, Y., Q. Zhang, Y. Ohishi, T. Shishido and K. Takehira; "Synthesis of V-MCM-41 by Template-ion Exchange Method and Its Catalytic Properties in Propane Oxidative Dehydrogenation," *Catal. Lett.*, **72**, 215–219 (2001)

Wang, Y., Y. Ohishi, T. Shishido, Q. Zhang, W. Yang, Q. Guo, H. Wan and K. Takehira; "Characterizations and Catalytic Properties of Cr-MCM-41 Prepared by Direct Hydrothermal Synthesis and Template-ion Exchange," *J. Catal*, **220**, 347–357 (2003)

Yonemitsu, M., Y. Tanaka and M. Iwamoto; "Metal Ion-Planted MCM-41. 1. Planting of Manganese (II) Ion into MCM-41 by a

Newly Developed Template-Ion Exchange Method," *Chem. Mater.*, **9**, 2679–2681 (1997)

Yoshiura, Y., N. Kijima, T. Hayakawa, K. Murata, K. Suzuki, F. Mizukami, K. Matano, T. Konishi, T. Oikawa, M. Saito, T. Shiojima, K. Wakui, G. Sawada, K. Sato, S. Matsuo and N. Yamaoka; "Catalytic Cracking of Naphtha to Light Olefins," *Catal. Surv. Japan*, **4**, 157–167 (2000)

Zhang, L., J. Deng, H. Dai and C. T. Au; "Binary Cr–Mo Oxide Catalysts Supported on MgO-coated Polyhedral Three-dimensional Mesoporous SBA-16 for the Oxidative Dehydrogenation of Iso-butane," *Appl. Catal. A,* **354**, 72–81 (2009)